ELSEVIER

Biophysical Chemistry 130 (2007) 1–9

Biophysical Chemistry

http://www.elsevier.com/locate/biophyschem

Visualization analysis of inter-fragment interaction energies of CRP–cAMP–DNA complex based on the fragment molecular orbital method

Ikuo Kurisaki [a,*], Kaori Fukuzawa [b,c], Yuto Komeiji [c,d], Yuji Mochizuki [c,e], Tatsuya Nakano [c,f], Janine Imada [g], Aneta Chmielewski [g], Stuart M. Rothstein [g], Hirofumi Watanabe [a,c], Shigenori Tanaka [a,c]

[a] *Graduate School of Science and Technology, Kobe University, 1-1, Rokkodai, Nada, Kobe 657-8501, Japan*
[b] *Mizuho Information and Research Institute, Inc., 2-3 Kanda Nishiki-cho, Chiyoda-ku, Tokyo 101-8443, Japan*
[c] *Japan Science and Technology Agency, CREST, Japan*
[d] *National Institute of Advanced Industrial Science and Technology, AIST, Central 2, Tsukuba 305-8568, Japan*
[e] *Department of Chemistry, Faculty of Science, Rikkyo University, 3-34-1 Nishi-Ikebukuro, Toshima-ku, Tokyo 171-8501, Japan*
[f] *Division of Safety Information on Drug, Food and Chemicals, National Institute of Health Sciences, 1-18-1 Kamiyoga, Setagaya-ku, Tokyo 158-8501, Japan*
[g] *Department of Chemistry and Centre for Biotechnology, Brock University, St. Catharines, Ontario, Canada L2S 3A1*

Received 6 April 2007; received in revised form 21 June 2007; accepted 25 June 2007
Available online 5 July 2007

Abstract

A visualization method for inter-fragment interaction energies (IFIEs) of biopolymers is presented on the basis of the fragment molecular orbital (FMO) method. The IFIEs appropriately illustrate the information about the interaction energies between the fragments consisting of amino acids, nucleotides and other molecules. The IFIEs are usually analyzed in a matrix form called an IFIE matrix. Analyzing the IFIE matrix, we detect important fragments for the function of biomolecular systems and quantify the strength of interaction energies based on quantum chemistry, including the effects of charge transfer, electronic polarization and dispersion force. In this study, by analyzing a protein–DNA complex, we report a visual representation of the IFIE matrix, a so-called IFIE map. We comprehensively examine what information the IFIE map contains concerning structures and stabilities of the protein–DNA complex.

Keywords: Fragment molecular orbital (FMO) method; Transcription factor; *Ab initio* quantum chemical calculation; DNA-binding protein; Sequence-specific recognition; Cyclic AMP receptor protein (CRP)

1. Introduction

Ab initio quantum chemical calculation is expected to give a wealth of insights into the physico-chemical properties of biomolecules, such as molecular interactions and chemical reactions, based on their electronic states. High-level *ab initio* calculations have been, however, possible only for small molecules or catalytic regions of enzymes because an enormous computation time was required even for a system consisting of less than 1000 atoms. In this context, fragment molecular orbital (FMO) method has recently been developed by Kitaura et al. [1–4] and has been the subject of a recent review [5]. The FMO method enables us to calculate electronic states of a huge system consisting of ~500 amino acid residues within realistic computation time, and the accuracy of FMO calculation has been confirmed in previous studies [5]. In the process of FMO calculation, inter-fragment interaction energies (IFIEs) can be simultaneously obtained. These can be interpreted as two-body interactions between fragments and are expected to provide

* Corresponding author. Tel.: +81 78 803 7991; fax: +81 78 803 7761.
E-mail addresses: kurisaki@insilico.h.kobe-u.ac.jp (I. Kurisaki), kaori.fukuzawa@mizuho-ir.co.jp (K. Fukuzawa), y-komeiji@aist.go.jp (Y. Komeiji), fullmoon@rikkyo.ac.jp (Y. Mochizuki), nakano@nihs.go.jp (T. Nakano), ji02fd@brocku.ca (J. Imada), achmiel2@uwo.ca (A. Chmielewski), srothste@brocku.ca (S.M. Rothstein), watanabe@radix.h.kobe-u.ac.jp (H. Watanabe), tanaka2@kobe-u.ac.jp (S. Tanaka).

0301-4622/$ - see front matter © 2007 Elsevier B.V. All rights reserved.
doi:10.1016/j.bpc.2007.06.011

useful information for analysis of intra- and inter-molecular interactions. We have already applied the FMO method to several biomacromolecular systems [6–9] and analyzed their IFIEs. For the cyclic AMP receptor protein (CRP)–cAMP–DNA system, we elucidated the sequence specificity of CRP–DNA binding, and the stability of the DNA duplex [6]. We also performed analysis of IFIEs for the estrogen receptor ligand-binding domain, and clarified the contributions of weak electrostatic and significant van der Waals dispersion interactions to ligand binding [7,8]. In addition, we developed the FMO-based method that analyzes the pattern of interaction of the receptor and ligand, and applied it to a docking study of pharmacophores of the human estrogen receptor [9].

However, the number of IFIE values obtained substantially increases in proportion to the square of the number of fragments: *e.g.*, 4950 IFIE values for a system containing 100 fragments. Thus, we have chosen some fragments that were expected to be important for biomacromolecular functions, and treated only a limited set of IFIEs for the analysis in previous studies, while a complete set of IFIEs would contain more information concerning the correlation with structural properties of biomacromolecules, such as positions of secondary structure and complex stability. In this study, we performed a comprehensive analysis of a whole set of IFIEs and extracted useful information by constructing colored IFIE maps. Here, we perform such an analysis of 29,890 IFIE values for the CRP–cAMP–DNA complex and report the correlation between the pattern of IFIEs and the structural properties of this biomolecular system.

2. Method

2.1. FMO method and IFIE

We employed FMO method to perform a high-level *ab initio* quantum chemical calculation at MP2/6-31G level [10,11] for biomacromolecular systems consisting of *ca.* 3000 atoms. The basic idea of the FMO method is to divide a large molecule into fragments, for example, a protein into amino acids (Fig. 1(A)). It should be noted that FMO fragments differ from the standard assignment for amino acid residues (Fig. 1(B)). A set of Schrödinger equations for each fragment and its pair are solved under the environmental electrostatic field until they converge self-consistently. The results are used to calculate the total energy of a system as shown below [6]:

$$E = \sum_{I>J}^{N} E_{IJ} - (N-2)\sum_{I}^{N} E_I \tag{1}$$

where N, E_I and E_{IJ} are the number of fragments, total energy of the monomer and that of the dimer, respectively.

This formulation of the total energy of the system can be transformed as follows [6]:

$$E = \sum_{I>J}^{N} \Delta E_{IJ} + \sum_{I}^{N} E'_I \tag{2}$$

$$\Delta E_{IJ} = (E'_{IJ} - E'_I - E'_J) + \mathrm{Tr}\left(\Delta P^{IJ} V^{IJ}\right) \tag{3}$$

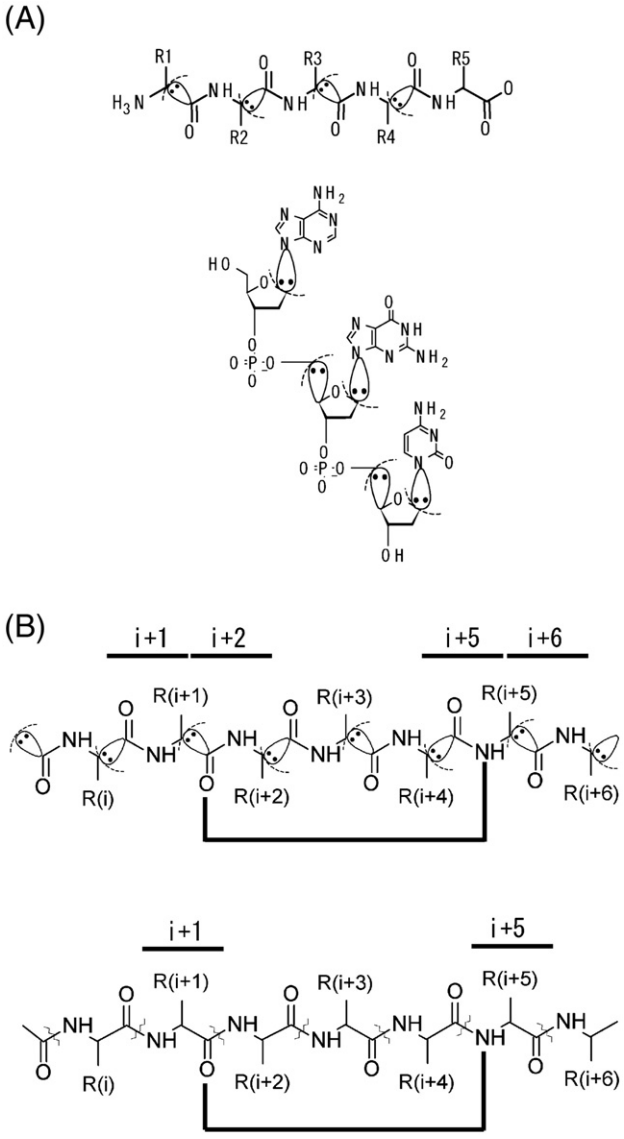

Fig. 1. (A) Fragmentation method of polypeptide (upper panel) and polynucleotide (lower panel). Each nucleotide is divided into a base and backbone (sugar and phosphate). (B) Residue assignment based on FMO definition (upper panel). Residue assignment based on standard definition (lower panel). These pictures were made by using ChemSketch [12].

where ΔP^{IJ}, V^{IJ}, E'_I and E'_{IJ} are the difference matrix, the environmental electrostatic potential for dimer IJ, monomer energy without environmental electrostatic potential, and dimer energy without environmental electrostatic potential, respectively. ΔE_{IJ} can be interpreted as an interaction energy between the Ith and Jth fragments, and we define ΔE_{IJ} as IFIEs. IFIEs are simultaneously obtained from FMO calculations, and are expected to give useful information about inter- and intra-molecular interactions.

2.2. The IFIE map

Treating a value of IFIE between the Ith and Jth fragment as an (I, J) element of a matrix, a set of IFIE values can be represented as a symmetric matrix. We call this the "IFIE matrix". Though this matrix contains precise information about IFIE

values, it is not convenient for comprehensive analysis over all the fragment pairs. To develop a more efficient way to analyze the IFIE matrix, we construct colored maps whose cells refer to the values of the IFIEs, a so-called "IFIE map". In the IFIE map, each cell is colored corresponding to the value of the IFIE matrix. The sign and strength of IFIEs are represented by color and hue, respectively. Red and blue colors correspond to negative and positive values, respectively. The deepness of the hue indicates the strength of the IFIEs. IFIE values between fragments joined by covalent bonds were neglected because of an artificial IFIE value (about −9000kcal/mol) associated with the bond detachment in the FMO calculation [5].

We next define a so-called difference IFIE matrix, whose elements are differences of IFIEs obtained under different conditions for the same fragment pair. Here we construct the difference IFIE matrix whose (I, J) components are equal to ΔE_{IJ} (complex) − ΔE_{IJ} (free), the difference of IFIEs between the complex and free structures. The IFIE maps display the IFIE matrix and the difference IFIE matrix. An IFIE map constructed from an IFIE matrix represents inter- and intra-molecular interactions, while that constructed from a difference IFIE matrix represents the change of intra-molecular interaction caused by the formation of the complex. All of the maps presented in this study were constructed using the graphical and data analysis software ORIGIN (http://www/orginlab.com/).

2.3. CRP–cAMP–DNA complex structure

CRP (also referred to as the "catabolite gene activator protein" or CAP) is a DNA-binding protein that acts as a sequence-specific transcription factor [13]. We obtained the initial atomic coorinates of the CRP–cAMP–DNA complex from the Protein Data Bank (PDB); the entry 1O3Q was used for preparing the structure [14]. The CRP–cAMP–DNA complex prepared for calculation consists of monomeric CRP containing 200 amino acid residues, the double-stranded DNA containing 11 base pairs (5′-$A_{-2}A_{-1}A_1A_2A_3T_4G_5T_6G_7A_8T_9$-3′) and one cAMP (Fig. 2(A)). We employ the complex of monomeric CRP–cAMP and DNA to obtain the calculation results within reasonable computational time, though CRP binds to DNA in the form of a homodimer.

The CRP–cAMP–DNA complex structure was relaxed using molecular dynamics simulation before quantum chemical calculation. Details of the simulation can be found in a previous study [6]. We obtained the results of the FMO calculation for the CRP–cAMP–DNA complex, CRP–cAMP and DNA at MP2/6-31G level, where the atomic coordinates of the CRP–cAMP and DNA were derived from the relaxed CRP–cAMP–DNA complex.

Using the DSSP method [16], we then defined the secondary structure of the relaxed CRP structure, six right-handed α-helices (indicated by α1–α6) and three anti-parallel β-sheets, S1, S2 and S3 (Fig. 2(B)).

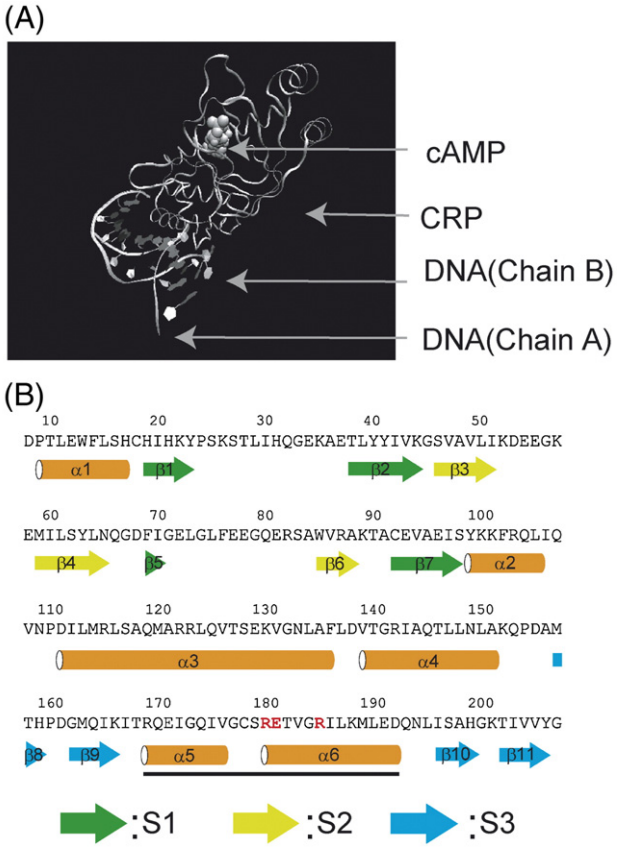

Fig. 2. Structure of cyclic AMP receptor protein (CRP). (A) Schematic representation of 3D structure of CRP monomer bound to DNA. CRP and DNA are represented by ribbon and cAMP by balls. This picture was prepared by using VMD program [15]. (B) Primary structure of CRP. Cylinder and arrow represent α-helix (α1–α6) and β-strand (β1–β11), respectively. Three anti-parallel β-sheets, S1, S2 and S3, were detected. Each β-sheet was distinguished by colors: green (S1), yellow green (S2), and cyan (S3). These assignments of secondary structure were defined by DSSP method [16]. The black line indicates the position of the DNA-binding helix-turn-helix motif. The red characters correspond to the glutamate and arginines identified as being important for binding to DNA. (For interpretation of the references to colour in this figure legend, the reader is referred to the web version of this article.)

3. Results and discussion

In a previous study [6] on the CRP–cAMP–DNA complex system, the IFIEs were directly analyzed for interactions of the CRP–cAMP with each base pair, the DNA duplex with each amino acid residue, and each base pair with each residue. However, dealing with raw IFIE values is inefficient for a comprehensive IFIE analysis of the DNA–cAMP–CRP complex. In this study, we construct the IFIE maps and visually extract information that could be inferred from them. These maps enable us to analyze IFIEs efficiently, and they actually contain useful information on the secondary structure of CRP and the stability of CRP–cAMP–DNA complex formation, as shown below.

3.1. Intra-molecular IFIE map

First, we construct the IFIE map with the data obtained from the FMO calculation at MP2/6-31G level for the CRP–cAMP–DNA complex system, focusing on the intra-molecular IFIEs (Figs. 3 and 4). In the intra-CRP IFIE (Fig. 3), we find three kinds of patterns: (1) parallel patterns to abscissa or ordinate

on the map, (2) a band pattern near and parallel to the diagonal line, and (3) band patterns roughly perpendicular to the diagonal line.

Pattern (1) is associated with Coulomb interactions, because charged residues can interact strongly with other distant amino acid residues. Patterns (2) and (3) are explained by the correspondence to protein secondary structures. Comparing these patterns with the positions of secondary structure (Fig. 2(B)), we find that pattern (2) corresponds to an α-helix and pattern (3) corresponds to an anti-parallel β-sheet. To analyze this correspondence in detail, we construct partial IFIE maps that contain the regions forming the secondary structures associated with α5, α6 and S1 (Fig. 5(A)).

In Fig. 5(B), partial IFIE maps show the regions forming α5 and α6. An α-helix is known to be stabilized by hydrogen bonds between the *i*th −CO and *i*+4th −NH groups according to the standard assignment of amino acid residues, while we use the different assignment for fragments as indicated in Fig. 1(B): the *i*th −CO and *i*+3rd −NH groups form hydrogen bonds. Thus, in Fig. 5(B), we then see that IFIEs between *i*th and *i*+3rd residues show a stabilization within the α-helix forming regions. Therefore we conclude that pattern (2) refers to α-helix forming regions. In addition, IFIEs between neighboring residues in the α-helix forming regions also show the stabilization (*i.e.*, *i*+1st or *i*+2nd residue for *i*th residue). This property corresponds to a well-known mechanism that a right-handed α-helix is also stabilized by the interaction of all constituent atoms of the main chain that are packed closely together [17].

On the other hand, in Fig. 5(C), partial IFIE maps show interactions between residues of each β-strand (upper), and inter-strand interaction between the β-strands contained in the S1 (lower). It is noted that β-sheets are stabilized by hydrogen bonds formed between β-strands. As expected, negative (red) points arranged perpendicular to the diagonal line are found in the region forming anti-parallel β-sheets (Fig. 5(C), lowers).

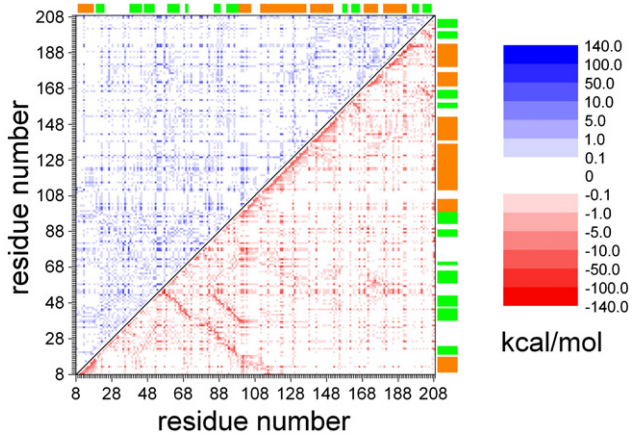

Fig. 3. An IFIE map for CRP forming the complex with DNA. An upper triangle is used to show the plots of positive IFIE values, whereas a lower triangle plots negative IFIE values. Numbers 8 to 207 correspond to those given for amino acid residues, whereas number 208 is used for cAMP. Orange rectangles along the axes indicate regions forming α-helices and green ones indicate regions forming β-strands. (For interpretation of the references to colour in this figure legend, the reader is referred to the web version of this article.)

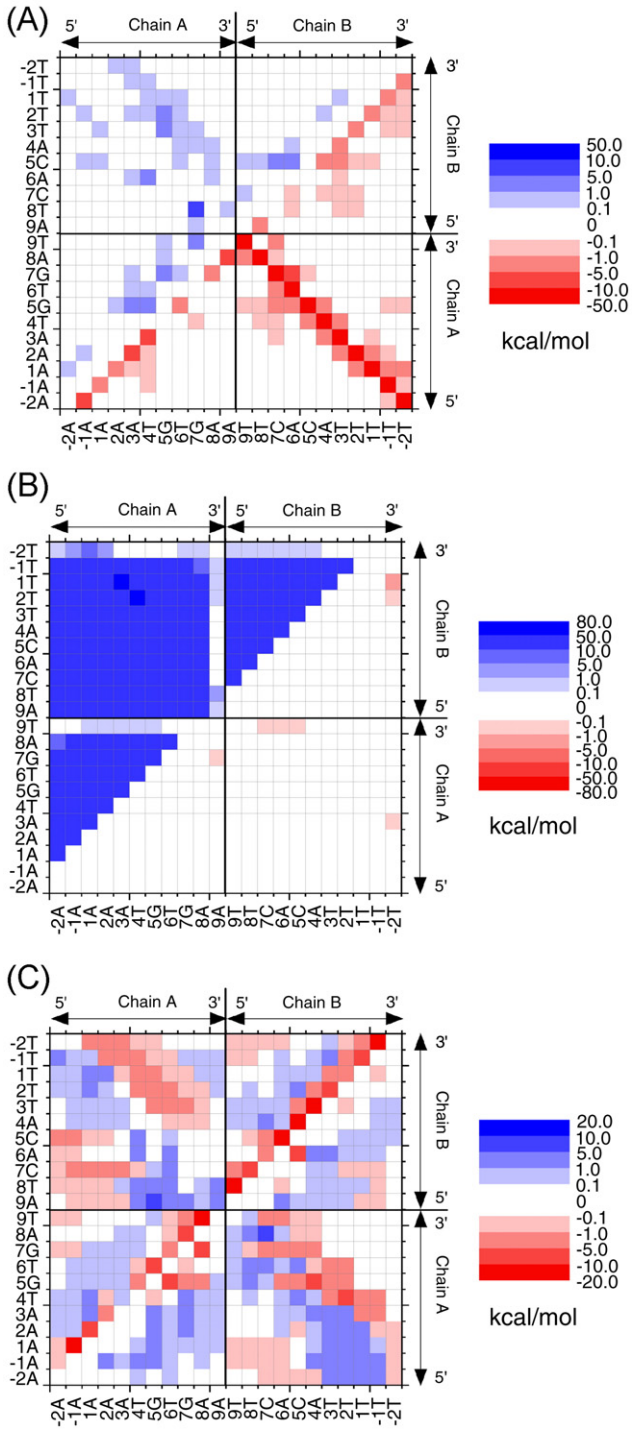

Fig. 4. IFIE maps for DNA forming the complex with CRP–cAMP. In (A) and (B), an upper triangle is used to show the plots of positive IFIE values, whereas a lower triangle plots negative IFIE values. (A), (B) Maps of IFIEs within DNA bases (A) and DNA backbone (sugar and phosphate) (B). (C) IFIEs between DNA base (abscissa) and DNA backbone (ordinate). (For interpretation of the references to colour in this figure legend, the reader is referred to the web version of this article.)

This indicates a correlation between pattern (3) and the regions forming β-sheets, while no common patterns are found in regions forming β-strands (Fig. 5(C), uppers). In addition, although the structure of CRP does not contain parallel β-sheets,

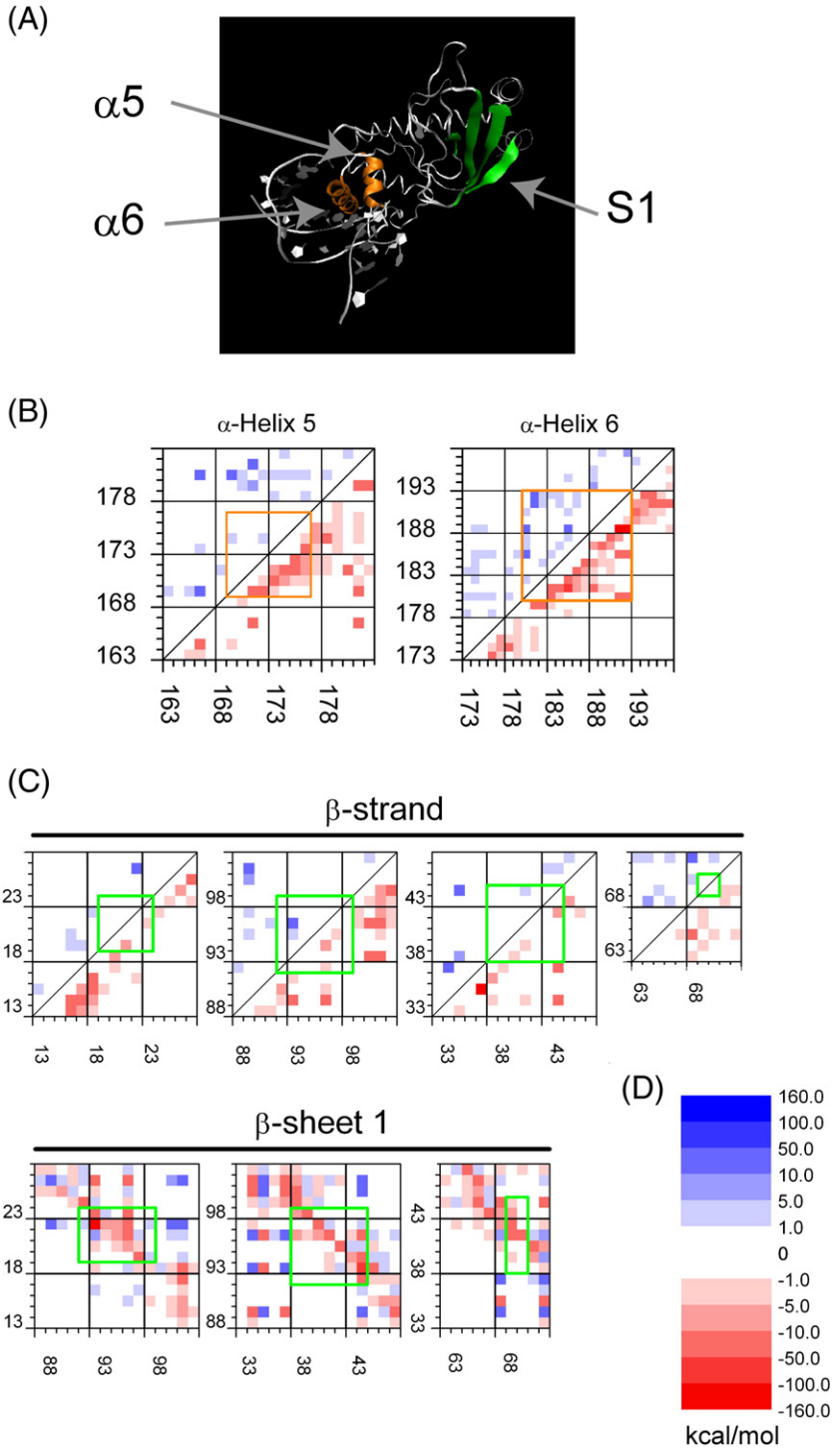

Fig. 5. IFIE maps focusing on regions forming secondary structures defined by DSSP method [13]. (A) α5, α6 and S1 are assigned in Fig. 2(B). This picture was prepared by using VMD program [15]. (B) IFIE maps corresponding to regions forming α5 (left) and α6 (right). Orange rectangles indicate α-helix forming regions. (C) Upper maps refer to regions forming β-strands within the S1 and lower ones indicate IFIEs between the β-strands. Green rectangles indicate regions forming β-strands (upper) and two β-strands located close to each other (lower). (D) Energy range of IFIE maps. (For interpretation of the references to colour in this figure legend, the reader is referred to the web version of this article.)

but it is expected that parallel β-sheets could be characterized by an IFIE pattern parallel to and distant from the diagonal line.

The intra-DNA IFIE map was divided into three partial maps: IFIEs between bases (Fig. 4(A)), backbones (Fig. 4(B)) and bases and backbones (Fig. 4(C)). Note that "Chain A" and "Chain B" in Fig. 4(A)–(C) correspond to those in Fig. 2(A). In Fig. 4(A), we find two kinds of patterns: (1) a band pattern near and parallel to the diagonal line, and (2) a band pattern roughly perpendicular to the diagonal line. Pattern (1) represents the stabilization by base–base intra-strand stacking interactions, whereas pattern (2) represents the hydrogen bonding between

Watson–Crick base pair (darker red pattern) and the base-base inter-strand stacking interactions.

In Fig. 4(B), most of IFIEs are blue-colored, thus representing a destabilization between backbones due to the negative charges associated with the phosphate groups of the DNA backbones, except for the 3′ terminus, which does not contain phosphates. In this case, no specific pattern is detected except the cluster of blue points.

Fig. 4(C) represents IFIEs between bases (abscissa) and backbones (ordinate). The band pattern near and parallel to the diagonal line represents base–backbone stabilization within the strand. Within Chain A (Chain B), IFIEs between *i*th (i+1st) DNA base and i+1st (*i*th) DNA backbone represent the stabilization, while concerning interactions between Chain A and Chain B, clusters of red and blue points are also found (note that "*i*" corresponds to the numbered entry of DNA; *e.g.*, the "1" in "1A"). Though they seemed to show specific patterns, we cannot find their correlation with any structural properties.

In summary, we can extract the specific patterns, and find the correlation between IFIEs and structural properties of biomacromolecules, from the intra-CRP–cAMP and intra-DNA base IFIE maps. Examining partial IFIE maps for the regions forming α-helices and anti-parallel β-sheets, we find correlations between the patterns on the IFIE map and the secondary structures of the protein, and the observed stabilization between neighboring residues in an α-helix corresponds to the well-known feature of right-handed α-helices. Furthermore, IFIE maps reflect the structural properties of DNA such as hydrogen bonding between Watson–Crick base pairs and base–base stacking. Finally, it remains to be done that we assign structural properties to the IFIEs between DNA bases and DNA backbones.

3.2. Intra-molecular difference IFIE map

To examine the effect of CRP–cAMP–DNA complex formation on intra-molecular stability, we computed the difference IFIE matrix whose components are given by ΔE_{IJ}(complex) − ΔE_{IJ}(free). In Fig. 6, specific patterns are found in the regions forming α-helices. For α1 and α3, clusters of blue points (indicating destabilization) are found, whereas for α2, α4, α5 and α6, clusters of red points (indicating stabilization) appear. On the other hand, positive and negative IFIE values coexisted in the region forming β-sheets.

In Fig. 7(A), we find the stabilization of base pairs 4T:A, 5G:C and 7G:C, which are parts of the conserved sequence recognized by CRP [11]. We also find a remarkable destabilization of intra-strand base–base stacking from 4T to 9A within DNA Chain A.

In Fig. 7(B), we find clusters of red and blue points. In Fig. 7 (C), from 4T to 9A in Chain A, the difference-IFIEs between *i*th base and i+1st (or i−1st) backbone represent a stabilization, while from 1T to 5C in DNA Chain B, the difference-IFIEs between *i*th base and i−1st (or i−2nd) backbone represent a stabilization. We cannot relevantly characterize the patterns observed in Fig. 7(B) and Fig. 7(C) based on DNA structural properties.

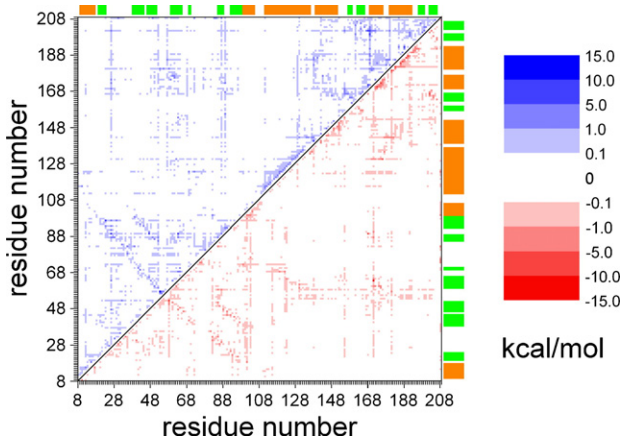

Fig. 6. Maps indicating the difference of IFIEs between CRP–cAMP forming complex with DNA and free molecules (CRP–cAMP). An upper triangle is used to show the plots of positive IFIE values, whereas a lower triangle plots negative IFIE values. Numbers 8 to 207 correspond to the numbers given for amino acid residues, whereas number 208 denotes cAMP. Orange rectangles along the axes indicate regions forming α-helices and green ones indicate regions forming β-strands as well as in Fig. 3. (For interpretation of the references to colour in this figure legend, the reader is referred to the web version of this article.)

The sum of difference IFIE values within a molecule represents the total change in intra-molecular stability induced by forming a complex. In CRP, the intra-molecular interaction is destabilized overall by 161kcal/mol. However, red and blue points coexist in the intra-CRP difference IFIE map, and cooperative changes of IFIEs are found within the regions forming α-helices. On the other hand, in the DNA, intra-molecular interaction is destabilized overall by 76kcal/mol, as was the case for CRP–cAMP, but the base pairs recognized by CRP, 4T:A, 5G:C and 7G:C, are stabilized upon forming the complex. This region-specific stabilization of IFIEs suggests that local intra-molecular stabilization is required for complex formation.

3.3. Inter-molecular IFIE map

Finally, we construct IFIE maps between CRP–cAMP and DNA for comprehensive analysis of the inter-molecular interaction (Fig. 8).

In the previous studies [14], the mechanism of CRP–DNA interaction was deduced from the CRP–cAMP–DNA complex structure. Arg-180, Glu-181 and Arg-185 were indicated as important residues involved in DNA binding. On the other hand, in our previous study [6], the interaction between CRP and DNA was revealed by analyzing IFIEs: the global effect of DNA on each amino acid and the effect of CRP on each base pair, each backbone pair or nucleotide pair, hydrogen bonding between Watson–Crick base pairs, base–base stacking interactions and the effect of amino acids on specific base pairs recognized by CRP, positions 4T:A to 8A:T.

In this study, we construct maps representing the IFIEs between CRP–cAMP and DNA, and perform a comprehensive analysis of the distribution of interactions between each amino

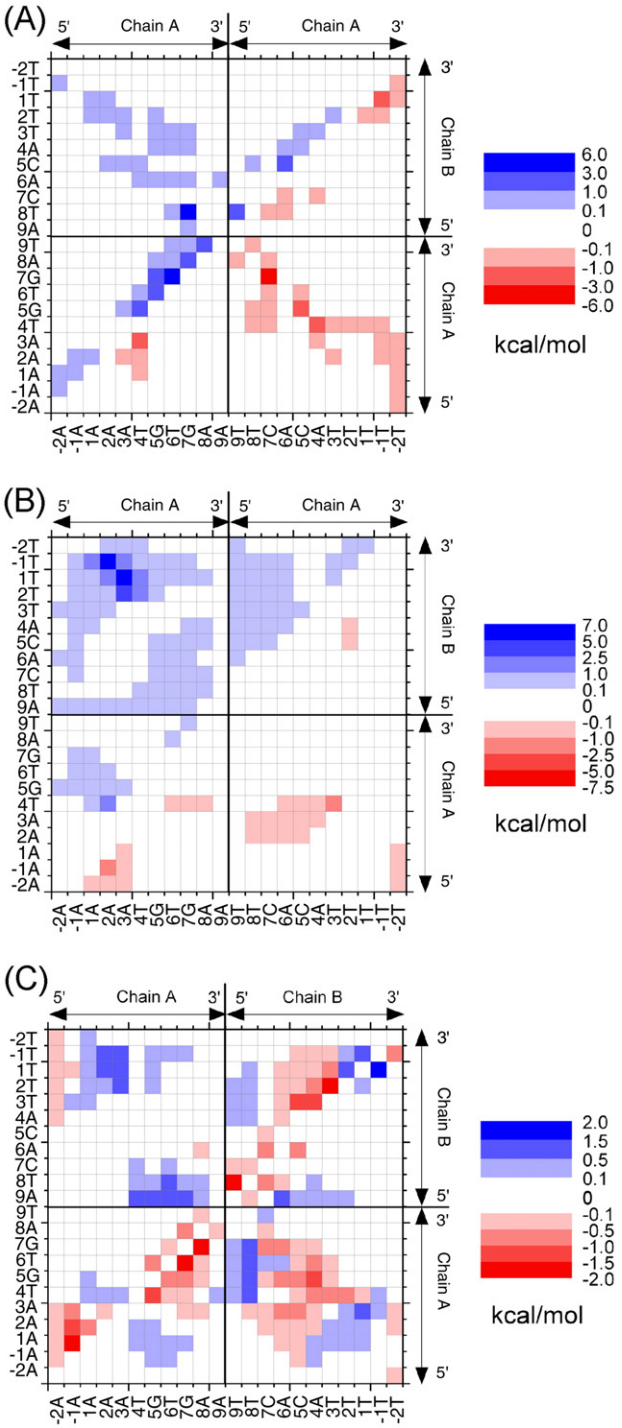

Fig. 7. Maps indicating the difference of IFIEs between DNA forming complex with CRP–cAMP and free molecules (DNA). In (A) and (B), an upper triangle is used to show the plots of positive IFIE values, whereas a lower triangle plots negative IFIE values. (A), (B) IFIE maps of difference-IFIEs within DNA bases in (A), DNA backbone (sugar and phosphate) in (B), and between DNA base (abscissa) and DNA backbone (ordinate) in (C). (For interpretation of the references to colour in this figure legend, the reader is referred to the web version of this article.)

acid and each nucleotide. We thus find specific interactions that are not inferred from the structural analysis.

At first, we examine the IFIE maps between CRP–cAMP and DNA bases. Previous structural studies have suggested the following interactions between amino acids and DNA bases: Arg-180 with 5G, Glu-181 with 7C and Arg-185 with 7G and 8T [14]. However, by analyzing the inter-IFIE maps, we identify more interactions than them. For DNA Chain A (Fig. 8(A), left), Arg-180 stabilizes 4T, 5G and 6T, while Arg-185 stabilizes 6T and 7G. For DNA Chain B (Fig. 8(A), center), Arg-180 stabilizes 6A, while Arg-185 stabilizes 8T and 9A. We also find that the IFIEs between Arg-180 and some bases represent destabilization: the IFIEs between this amino acid and 5C and 7C in Chain B, for example. Glu-181 also strongly interacts with DNA bases. From the IFIE map, we reveal that the IFIEs between this residue and DNA bases in Chain A represent a remarkable destabilization from 3A to 9T, while IFIEs with DNA bases in Chain B, from 6T to 8C, represent a stabilization.

Considering the IFIEs between amino acids and DNA base pairs (Fig. 8(A), right), Arg-180 interacts with 4T:A, 5G:C and 6T:A, and Arg-185 interacts with 7G:C, 8A:T and 9T:A. Glu-181 is stabilized by the interaction with 7G:C and 8A:T, but destabilized by the interaction with 5G:C. In addition, other amino acids within the DNA-binding helix are stabilized by the interaction with DNA bases, though their IFIEs are weaker than those between the arginines and DNA bases.

Next, we examine the IFIE maps between amino acids and DNA backbones (Fig. 8(B)). Due to the negative charges of the DNA backbones, Coulomb interactions between a charged residue and a DNA backbone are remarkably dominant. We can identify these interactions as horizontal lines. On the other hand, we find clusters of red spots composed of IFIEs between DNA backbones and uncharged amino acids within the DNA-binding helix-turn-helix motif, though the strengths of the IFIEs are weaker than those between DNA backbones and charged amino acids.

In summary, we performed a comprehensive analysis of IFIEs between the CRP–cAMP and DNA. The IFIE maps represented the distribution of interactions between amino acids and nucleotides in this system. We found amino acid–DNA base interactions that were not deduced by the previous structural studies, concerning not only on Arg-180, Glu-181 and the Arg-185 but also other amino acids within the DNA-binding helix-turn-helix motif. Coulomb interactions between charged amino acids and the DNA backbones are remarkable, and interactions between uncharged amino acids within DNA-binding domain and the DNA backbones also contribute to the stability of complex.

4. Conclusions

We developed a visualization method for IFIEs based on the *ab initio* FMO method, performed a comprehensive analysis of a complete set of IFIE values, and extracted useful information from IFIE maps. First, we showed that the patterns of IFIEs are correlated with specific structures of proteins and DNA. The intra-IFIE map of CRP indicates the presence of α-helices and β-sheets, and the intra-IFIE map of DNA bases reveals hydrogen bonding between Watson–Crick base pairs, and base–base stacking. Second, we found that complex formation induces a change of intra-IFIEs that correlates with structure. Calculating difference-IFIEs, we revealed that stabilization and destabilization are markedly observed in the regions forming α-helices, and

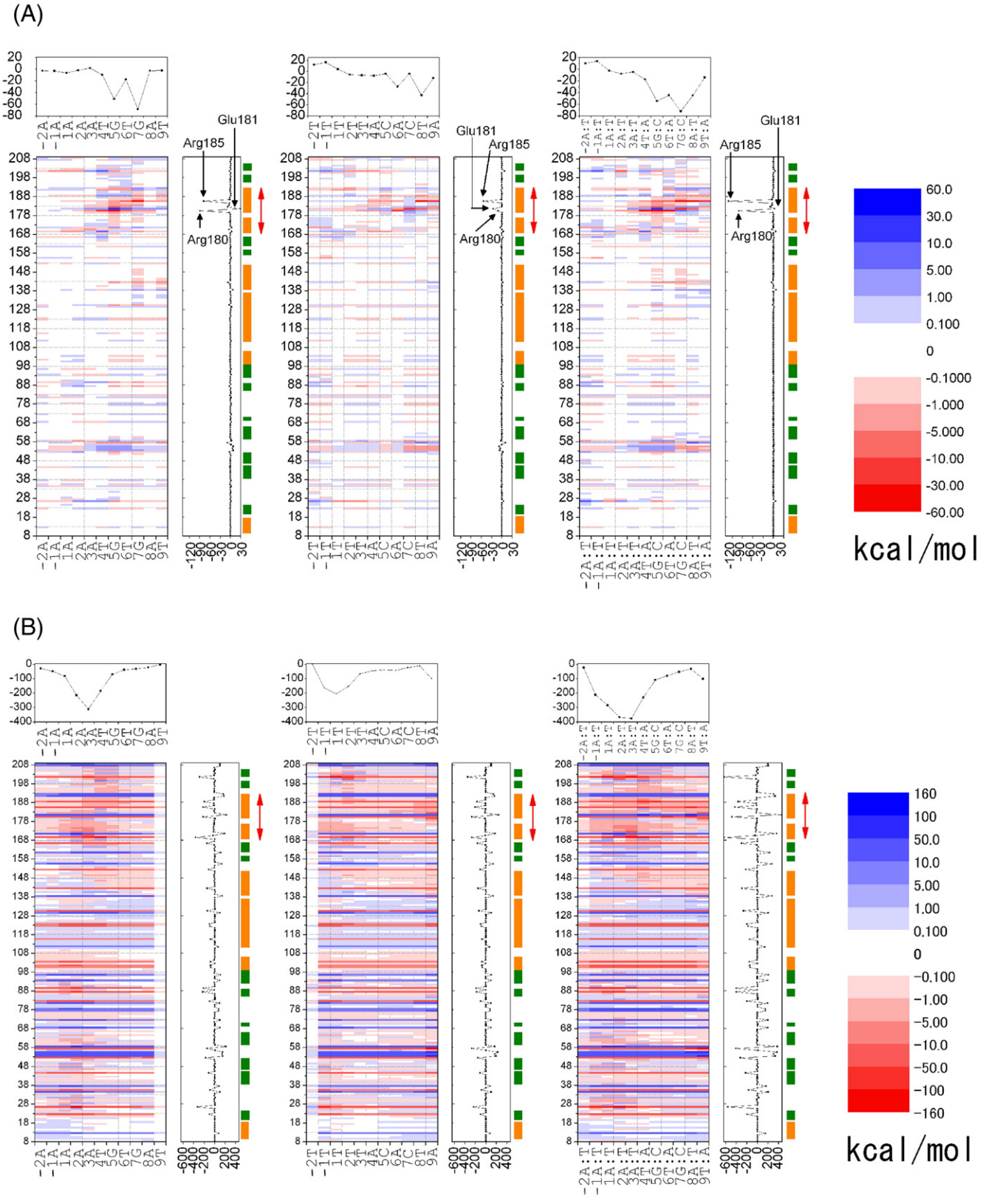

Fig. 8. Maps representing the IFIEs between CRP and DNA bases (upper panels) and between CRP and DNA backbones (lower panels). Left panels indicate IFIEs between CRP and Chain A, center panels IFIEs between CRP and Chain B, and right panels IFIEs between CRP and the pair of chains. Note that "Chain A" and "Chain B" correspond to those in Fig. 2A. Double head arrows indicate the position of the DNA-binding helix-turn-helix motif. The numbers along the ordinate denote residue numbers: the numbers 8 to 207 are assignments given to amino acid residues, whereas the entry number 208 is used to denote cAMP. In addition to the IFIE map, the sum of IFIEs is also indicated above and on the right side of each IFIE map.

in DNA bases recognized by CRP. Finally, we provided a detailed analysis of the distribution of IFIEs between CRP–cAMP and DNA, mainly by focusing on the important amino acid residues identified as being involved in DNA binding. We uncovered specific interactions, which had not been deduced from previous structural studies of the CRP–cAMP–DNA complex system; interactions between DNA backbones and uncharged amino acids, found as cluster patterns within the DNA-binding helix-turn-helix motif, contribute to the stabilization of the CRP–cAMP–DNA complex as well as those between charged amino acids and DNA backbones.

In this study, we proposed an efficient method to extract useful information from an IFIE matrix and showed some examples. We here employed this method for IFIEs obtained from quantum chemical calculation of biomolecules in gas phase, not in realistic system, requiring caution when compared with experiments. However, the method can be applied to IFIEs obtained from calculations of more realistic systems such as biomolecules in water solvent as well, whose example is FMO–MP2 calculation for cisplatin–DNA complex as reported previously [18]. In addition, to find and exploit more information buried in a complete set of IFIEs, it would be useful to examine the correlation of IFIE patterns with experimental or other simulation results such as the energy decomposition analyses based on semi-empirical quantum chemical method [19] and classical trajectory obtained from molecular dynamics simulation [20]. Research in this direction would be a future task.

Acknowledgment

This work was supported by the Core Research for Evolutional Science and Technology (CREST) project of the Japan Science and Technology Agency (JST). We thank Prof. Minoru Sakurai of Tokyo Institute of Technology, Prof. Kuniyoshi Ebina of Kobe University, Dr. Shinji Amari of University of Tokyo and Mr. Bryan VanSchouwen of Brock University for useful comments.

References

[1] K. Kitaura, T. Sawai, T. Asada, T. Nakano, M. Uebayasi, Pair interaction molecular orbital method: an approximate computational method for molecular interactions, Chem. Phys. Lett. 312 (1999) 319–324.
[2] K. Kitaura, E. Ikeo, T. Asada, T. Nakano, M. Uebayasi, Fragment molecular orbital method: an approximate computational method for large molecules, Chem. Phys. Lett. 313 (1999) 701–706.
[3] T. Nakano, T. Kaminuma, T. Sato, Y. Akiyama, M. Uebayasi, K. Kitaura, Fragment molecular orbital method: application to polypeptides, Chem. Phys. Lett. 318 (2000) 614–618.
[4] T. Nakano, T. Kaminuma, T. Sato, K. Fukuzawa, Y. Akiyama, M. Uebayasi, K. Kitaura, Fragment molecular orbital method: use of approximate electrostatic potential, Chem. Phys. Lett. 351 (2002) 475–480.
[5] D.G. Fedorov, K. Kitaura, Theoretical development of the fragment molecular orbital (FMO) method, in: E.B. Starikov, J.P. Lewis, S. Tanaka (Eds.), Modern Methods for Theoretical Physical Chemistry of Biopolymers, Elsevier, 2006, pp. 3–38.
[6] K. Fukuzawa, Y. Komeiji, Y. Mochizuki, A. Kato, T. Nakano, S. Tanaka, Intra- and intermolecular interactions between cyclic-AMP receptor protein and DNA: ab initio fragment molecular orbital study, J. Comput. Chem. 27 (2006) 948–960; ibid. 28 (2007) 2237–2239.
[7] K. Fukuzawa, K. Kitaura, M. Uebayasi, K. Nakata, T. Kaminuma, T. Nakano, Ab initio quantum mechanical study of the binding energies of human estrogen receptor-α with its ligands: an application of fragment molecular orbital method, J. Comput. Chem. 26 (2005) 1–10.
[8] K. Fukuzawa, Y. Mochizuki, S. Tanaka, K. Kitaura, T. Nakano, Molecular interactions between estrogen receptor and its ligand studied by the ab Initio fragment molecular orbital method, J. Phys. Chem., B. 110 (2006) 16102–16110; ibid. 110 (2006) 24276.
[9] S. Amari, A. Aizawa, Z. Junwei, K. Fukuzawa, Y. Mochizuki, Y. Iwasawa, K. Nakata, H. Chuman, T. Nakano, VISCANA: visualized cluster analysis of protein-ligand interaction based on the ab initio fragment molecular orbital method for virtual ligand screening, J. Chem. Inf. Model. 46 (2006) 221–230.
[10] Y. Mochizuki, T. Nakano, S. Koikegami, S. Tanimori, Y. Abe, U. Nagashima, K. Kitaura, A parallelized integral-direct second-order Mϕller–Plesset perturbation theory method with a fragment molecular orbital scheme, Theo. Chem. Acc. 112 (2004) 442–452.
[11] Y. Mochizuki, S. Koikegami, T. Nakano, S. Amari, K. Kitaura, Large scale MP2 calculations with fragment molecular orbital scheme, Chem. Phys. Lett. 396 (2004) 473–479.
[12] ACD/ChemSketch Freeware, Version 10.00 (Advanced Chemistry Development, Inc.: Toronto, ON, Canada, www.acdlabs.com, 2006).
[13] A. Gunasekera, Y.W. Ebright, R.H. Ebright, DNA sequence determinants for binding of the *Escherichia coli* catabolite gene activator protein, J. Biol. Chem. 267 (1992) 14713–14720.
[14] S. Chen, J. Vojtechovsky, G.N. Parkinson, R.H. Ebright, H.M. Berman, Indirect readout of DNA sequence at the primary-kink site in the CAP–DNA complex: DNA binding specificity based on energetics of DNA kinking, J. Mol. Biol. 314 (2001) 63–74.
[15] W. Humphrey, A. Dalke, K. Schulten, VMD — visual molecular dynamics, J. Mol. Graph. 14.1 (1996) 33–38.
[16] W. Kabsch, C. Sander, Dictionary of protein secondary structure: pattern recognition of hydrogen-bonded and geometrical features, Biopolymers 22 (1983) 2577–2637.
[17] K. Hamaguchi, The Protein Molecule, Japan scientific societies press, Japan, 1992.
[18] T. Ishikawa, Y. Mochizuki, T. Nakano, S. Amari, H. Mori, H. Honda, T. Fujita, H. Tokiwa, S. Tanaka, Y. Komeiji, K. Fukuzawa, K. Tanaka, E. Miyoshi, Fragment molecular orbital calculations on large scale systems containing heavy metal atom, Chem. Phys. Lett. 427 (2006) 159–165.
[19] K. Raha, A.J. van der Vaart, K.E. Riley, M.B. Peters, L.M. Westerhoff, H. Kim, K.M. Merz Jr., Pairwise decomposition of residue interaction energies using semiempirical quantum mechanical methods in studies of protein–ligand interaction, J. Am. Chem. Soc. 127 (2005) 6583–6594.
[20] G. Tiana, F. Simona, G.M. De Mori, R.A. Broglia, G. Colombo, Understanding the determinants of stability and folding of small globular proteins from their energetics, Protein Sci. 13 (2004) 113–124.